Kinetics of CO_x Formation in the Homogeneous Metal/Bromide-Catalyzed Aerobic Oxidation of *p*-Xylene

WEIZHEN SUN,[1] MEIYING AN,[1] WEIMIN ZHONG,[2] LING ZHAO[1]

[1]*State Key Laboratory of Chemical Engineering, East China University of Science and Technology, Shanghai* 200237, *People's Republic of China*
[2]*Key Laboratory of Advanced Control and Optimization for Chemical Processes, Ministry of Education, East China University of Science and Technology, Shanghai* 200237, *People's Republic of China*

Received 31 May 2011; revised 30 August 2011, 16 December 2011; accepted 4 January 2012

DOI 10.1002/kin.20724
Published online 5 March 2012 in Wiley Online Library (wileyonlinelibrary.com).

ABSTRACT: The homogeneous metal/bromide-catalyzed aerobic oxidation of *p*-xylene with different catalyst concentrations was carried out, and the formation kinetics of CO_x including CO_2 and CO was measured. The simplified elementary steps for the formation of CO_x were summarized, on the basis of which the kinetic model of CO_x formation was established. The model calculations were in good agreement with the experimental data for the CO_2 formation and also successfully captured the first peak of the CO formation rate as a function of time. The obtained rate constants have narrow confidence intervals, among which only k_1 and k_2 are the adjustable parameters for different catalyst conditions. The decarboxylation of the carboxyl group in aromatic acid, the oxidation of the aryl radical, and the destruction of acetic acid are

Correspondence to: Ling Zhao; e-mail: zhaoling@ecust.edu.cn.
Contract grant sponsor: The Program for Changjiang Scholars and Innovative Research Team in University.
Contract grant number: IRT0721.
Contract grant sponsor: The 111 Project.
Contract grant number: B08021.
Contract grant sponsor: The National Natural Science Foundation of China.
Contract grant number: 60804029.
Contract grant sponsor: The Fundamental Research Funds for the Central Universities.

the major sources of CO_2. The formation of CO mainly results from the destruction of acetic acid and the oxidation of the aryl radical. © 2012 Wiley Periodicals, Inc. Int J Chem Kinet 44: 277–283, 2012

INTRODUCTION

The liquid-phase oxidation of hydrocarbons by molecular oxygen is of vital scientific, technological, and commercial importance [1]. It is also called autoxidation because these reactions proceed spontaneously even at lower temperatures. Through autoxidation, a number of hydrocarbons from fossil fuel, notably *p*-xylene (PX), cumene, ethylbenzene, and cyclohexane, are directly oxidized into important oxygenated chemicals. In autoxidation, the homogeneous metal/bromide catalyzed aerobic (HMBCA) oxidation of hydrocarbons originally invented by Mid-Century Corporation occupies an important position, because of the high activity of catalyst, high selectivity over a very large operating temperature range and wide applications. One of the most popular catalysts in HMBCA oxidation, perhaps the most important, is the combination of cobalt (Co), manganese (Mn), and bromide (Br). There is a complex synergy between these catalyst components [2,3].

Like most other chemical reactions, some by-products are encountered in the HMBCA oxidation despite its high selectivity. Taking the oxidation of PX to terephthalic acid as an example, 32 different by-products have been reported [4]. Three of them are generated in higher yield than 0.1%, including carbon dioxide (CO_2), methyl acetate, and an aromatic acid containing one less carboxylic group. In the generation of the last two by-products, that is, methyl acetate and aromatic acid, CO_2 and/or carbon monoxide (CO) are the concomitants. So, it is natural that the formation of CO_x (CO_2 and CO) can be used to estimate side reactions in HMBCA oxidation. To some extent, the possible mechanism for the formation of by-products in HMBCA oxidation has been discussed [5–7]. Even some kinetic data can be found concerning the destruction of acetic acid in PX oxidation [8]. However, kinetic models concerning the formation of CO_x are less often reported in the open literature.

In this work, the kinetics of CO_x formation in PX oxidation was first measured under the industrial conditions. Also, the kinetic model was established on the basis of elementary steps, that is, free radical reaction mechanism, and the rate constants were determined.

EXPERIMENTAL

The PX oxidation process was semicontinuously carried out, in which the reactant PX, catalyst, and solvent (i.e., a mixture of acetic acid and water with 5% mass concentration of water) were put into the reactor and the high-pressure air was introduced continuously. In each experimental run, the mixture of PX, catalyst (cobalt acetate, manganese acetate, and hydrogen bromide), and solvent was first put into the reactor. When the temperature and pressure were enhanced to a set point in the inert nitrogen atmosphere, air was introduced into the reactor and the reaction was started. The experiments were performed at a pressure of 1.3 MPa and a temperature of 453 K and with different catalyst concentrations.

The experimental setup is shown in Fig. 1. The reactor has a volume of 1 L, is made of titanium, and is equipped with four baffles. To remove the reaction heat, a cooling coil is installed inside the reactor. The oil flow in the cooling coil is adjusted by an oil pump with a PID control. The reaction temperature is monitored by a thermocouple and controlled by a computer. At certain intervals ranging from 30 to 300 s, depending on the rate of reaction, samples are taken for analysis. A more detailed description of the experimental procedure can be found in the literature [9,10]. A combined method based on chromatography was used to analyze the liquid-phase products [11].

For gas-phase products, tail gas from the reactor was analyzed by an oxygen analyzer and two infrared gas analyzers. The oxygen analyzer was used to measure the oxygen content by the thermal magnetic property of oxygen, and an infrared gas analyzer with the wavelength of 1–25 μm was used to measure the contents of CO and CO_2, respectively. The formation rate of CO_x is defined by

$$r_{CO_x} = \frac{[CO_x] \times Q_{Air} \times 0.79}{(1 - [O_2] - [CO_x]) \times 22.4 \times M_{sol}} \quad (1)$$

where $[CO_x]$ and $[O_2]$ stand for the molar content of CO_x and O_2 in tail gas, respectively, Q_{Air} represents volume flow of air under normal conditions, and M_{sol} is the total mass of the liquid-phase solution in a reactor.

REACTION PATHS FOR CO_X FORMATION

Similar to the main reaction in PX oxidation, the formation of CO_x follows the free radical reaction mechanism. Under the attack of free radicals and metals in the high oxidation state, aromatic acid and acetic acid tend to produce CO_x.

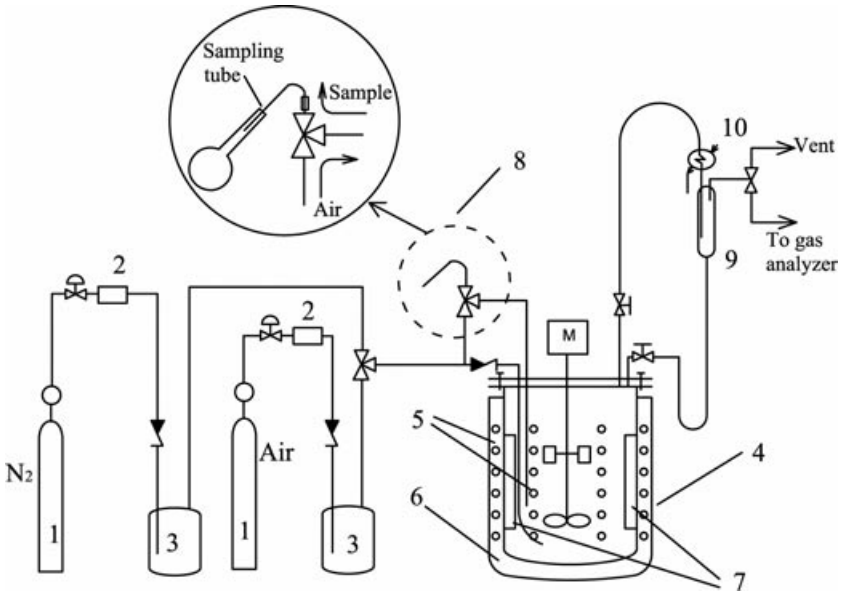

Figure 1 Schematic diagram of experimental setup: 1, cylinder; 2, flow controller; 3, acetic acid tank; 4, reactor; 5, cooling coil; 6, oil-bath; 7, baffle; 8, sampler; 9, reflux splitter; and 10, condenser.

The first main source of CO_x is the decarboxylation of aromatic acid, which releases carbon dioxide. The decarboxylation usually refers to the reaction of a compound with at least one carboxylic acid, by which a carbon atom is removed from a carbon chain. Heating is usually required because the reaction is less favorable at low temperatures. The reaction mechanism of decarboxylation can be complicated. Generally, the decarboxylation of aliphatic carboxylic acids is strongly dependent on the group attached and the bond type at the β-position [12,13]. For aromatic acids, the aromatic ring acts as an electron sink that dissipates the developing negative charge on the α-carbon atom [13]. In the presence of high-valent transition metal, the aromatic acid is decarboxylated as follows [5]:

$$\text{Ar-COOH} + \text{M}^{\text{III}} \xrightarrow{k_1} \text{Ar}^{\bullet} + \text{CO}_2 + \text{M}^{\text{II}} + \text{H}^{+} \quad (2)$$

where Ar- represents an aryl group and M stands for the transition metal. The aryl radical $Ar^{\bullet}$ from reaction (2) is known to be rapidly oxidized to a phenol or cresol, which is then completely oxidized to more CO_x [14]. The existence of phenol had been identified, and it was believed to be constantly formed by reaction (3) [4]. But it is not very clear about a detailed mechanism concerning the oxidation of the aryl radical to the phenol in the autoxidation of PX. While in the oxidation of benzene, the phenyl radical can react solely with O_2 to mainly form a phenoxy radical [15]. The phenoxy radical will be further converted to a phenol in the presence of H_2O. The conversion of the methyl phenol to quinone can proceed in the participation of the peroxy radical [14], but the exact reaction pathway is not well documented:

$$\text{CH}_3\text{Ar}^{\bullet} \xrightarrow{+\text{O}_2} \text{CH}_3\text{Ar-OH} \quad (3)$$

$$\text{CH}_3\text{Ar-OH} \xrightarrow{+\text{peroxy radical}} \text{Quinones} \xrightarrow{k_6,\, k_7} 7\text{CO}_2, 7\text{CO} \quad (4)$$

The competitive reaction of step (3) is the following step (5), which should be the source of benzoic acid and the benzene. In step (5), RH represents hydrocarbon or aldehyde:

$$\text{Ar}^{\bullet} + \text{RH} \xrightarrow{k_8} \text{Ar-H} \quad (5)$$

The oxidative decomposition of acetic acid proceeds by the way of co-oxidation with aromatic hydrocarbon. Alkylperoxy radicals generated in the PX oxidation attack on the molecule of acetic acid [7]:

$$\text{CH}_3\text{COOH} + \text{ROO}^{\bullet} \xrightarrow{k_9} \text{ROOH} + \text{CH}_3\text{COO}^{\bullet} \quad (6)$$

where $ROO^{\bullet}$ stands for the alkylperoxy radical, including all of the radicals generated in the PX oxidation. The radical $CH_3COO^{\bullet}$ is unstable, decomposing immediately to CO_2:

$$\text{CH}_3\text{COO}^{\bullet} \rightarrow {}^{\bullet}\text{CH}_3 + \text{CO}_2 \quad (7)$$

Theoretically, the following step also proceeds, competing against step (6):

$$\text{Ar-COOH} + \text{ROO}^{\bullet} \xrightarrow{k_{10}} \text{ROOH} + \text{Ar-COO}^{\bullet} \quad (8)$$

The destruction of acetates is another main source of CO_x. In the catalyst system, where there is only cobalt acetate or a combination of cobalt acetate and bromide, the reaction of acetate with Co(III) is important and should be considered. But when manganese acetate is added to this system, the steady-state concentration of Co(III) is much reduced because of a rapid reaction of Co(III) with manganese(II) [3,16]. So, in the catalyst system of Co/Mn/Br, the reaction of acetate with Mn(III) is predominant. The mechanism of destruction depends on the nature of the metal [8]. In the case of Mn(III), a carbon-centered radical is formed:

$$\text{Mn(CH}_3\text{COO)}_3 \xrightarrow{k_2} \text{Mn(CH}_3\text{COO)}_2 + {}^{\bullet}\text{CH}_2\text{COOH} \quad (9)$$

The radical $^{\bullet}CH_2COOH$ interacts with O_2 rapidly and further attacks the H atom in RH:

$$^{\bullet}\text{CH}_2\text{COOH} + \text{O}_2 \rightarrow {}^{\bullet}\text{OOCH}_2\text{COOH} \quad (10)$$

$$^{\bullet}\text{OOCH}_2\text{COOH} + \text{RH} \xrightarrow{k_4} \text{HOOCH}_2\text{COOH} + \text{R}^{\bullet} \quad (11)$$

The $HOOCH_2COOH$ is further converted to the products of complete and incomplete oxidation, that is, CO, CO_2, formaldehyde, and formic acid [8]:

$$\text{HOOCH}_2\text{COOH} \xrightarrow{k_3, k_5 \cdots} \text{CO, CO}_2, \text{HCOH, HCOOH, H}_2\text{O} \quad (12)$$

Theoretically, the formation of CO is also contributed by the decarbonylation of the aldehyde group or the carbonyl radical in the phenyl ring:

$$\text{Ar-CHO} + \text{Co}^{\text{III}} \xrightarrow{k_{11}} \text{Ar}^{\bullet} + \text{CO} + \text{Co}^{\text{II}} + \text{H}^{+} \quad (13)$$

$$\text{Ar-CO}^{\bullet} \xrightarrow{k_{12}} \text{Ar}^{\bullet} + \text{CO} \quad (14)$$

where $Ar\text{-}CO^{\bullet}$ stands for the carbonyl radical generated in the PX oxidation. However, these two reaction steps were reported not to be important in the autoxidation of aromatic aldehyde, because the decarbonylation of benzaldehyde is very little as compared with that of aliphatic aldehyde formed as intermediates during the oxidation of acetic acid [14]. Accordingly, Eqs. (13) and (14) will not be involved in the model.

MODEL SOLVING AND SIMPLIFICATIONS

Considering these rate-determining steps and assuming other steps to be instantaneous, the formation kinetics of CO_x can be readily formulated. To obtain the rate constants, the following object function was used:

$$\text{obj} = \sum_{i=1}^{m} \left(r_i^{\text{exp}} - r_i^{\text{cal}}\right)^2 \quad (15)$$

where r_i^{exp} represents the experimental data of CO_2 and CO based on Eq. (1), r_i^{cal} stands for the calculated value based on kinetic model equations (16)–(21), and m is the number of the experimental data. The seeking of the optimum rate constants was achieved by the function *lsqnonlin* as in the MATLAB (Natick, MA, USA) computational platform.

The preliminary fitting results show that some of estimated rate constants are much lower than their respective confidence intervals, that is, the constants in Eqs. (6) and (8). So, the formation of CO_x by both steps (6) and (8) will not be taken into account in the kinetic model to make the confidence intervals narrow. It is found that after these adjustments the agreement between experiments and model calculation changes very little, and the confidence intervals become narrower. As a result, the kinetic model for CO_x formation can be written as follows:

$$\frac{\text{d}[^{\bullet}\text{OOCH}_2\text{COOH}]}{\text{d}t} = k_2 - k_4 \times [^{\bullet}\text{OOCH}_2\text{COOH}][\text{RH}] \quad (16)$$

$$\frac{\text{d}[\text{Ar}^{\bullet}]}{\text{dt}} = k_1 \times [\text{Ar-COOH}] - k_6 \times [\text{Ar}^{\bullet}] - k_7[\text{Ar}^{\bullet}] \quad (17)$$

$$\frac{\text{d}[\text{HOOCH}_2\text{COOH}]}{\text{d}t} = k_4 \times [^{\bullet}\text{OOCH}_2\text{COOH}][\text{RH}] - k_3 \times [\text{HOOCH}_2\text{COOH}] - k_5 \times [\text{HOOCH}_2\text{COOH}] \quad (18)$$

$$\frac{\text{d}[\text{CO}_2]}{\text{d}t} = k_1 \times [\text{Ar-COOH}] + k_6 \times [\text{Ar}^{\bullet}] \times 7 + k_5 \times [\text{HOOCH}_2\text{COOH}] \quad (19)$$

$$\frac{\text{d}[\text{CO}]}{\text{d}t} = k_3 \times [\text{HOOCH}_2\text{COOH}] + k_7 \times [\text{Ar}^{\bullet}] \times 7 \quad (20)$$

$$t = 0, [^{\bullet}\text{OOCH}_2\text{COOH}] = 0, [\text{HOOCH}_2\text{COOH}] = 0, [\text{CO2}] = 0, [\text{CO}] = 0. \quad (21)$$

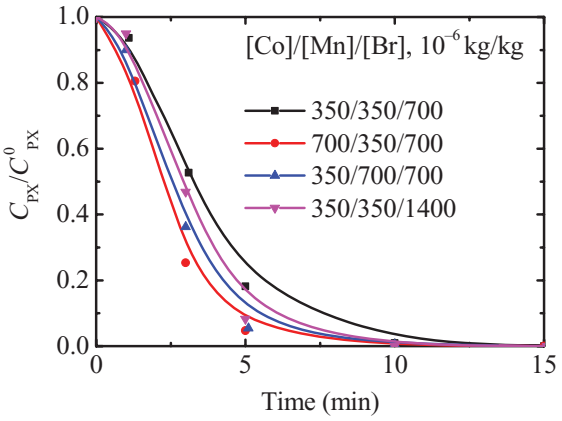

Figure 2 Disappearance of PX with time at different catalyst composition and concentrations. $T = 465$ K.

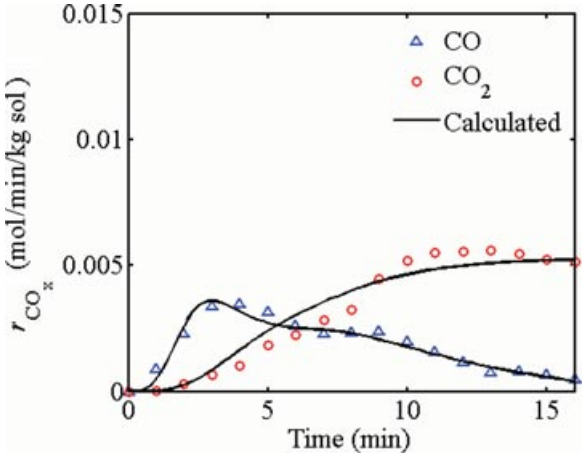

Figure 3 Model fitting to the formation rate of CO_x. [Co]/[Mn]/[Br]: 350/350/700 10^{-6} kg/kg; $T = 465$ K.

Equations (16)–(21) are ordinary differential equations and can be solved by *ode45* in MATLAB.

RESULTS AND DISCUSSION

According to the elementary steps in CO_x formation, the formation kinetics of CO_x is much related to the main reaction of PX oxidation, including intermediates and free radicals. Their concentration profiles can be readily calculated from the main reaction kinetics of PX oxidation [9,10] when the model parameter(s) is known. To determine the rate constants in PX oxidation kinetics, the liquid phase was also sampled in the experiments. The disappearance of PX with time in different catalyst composition and concentrations is shown in Fig. 2. According to the main reaction kinetics of PX oxidation, there are six model parameters, in which only the initiation rate constant k'_1 is adjustable when the catalyst composition or concentration varies. The values of k_1 and k_2–k_6 are listed in Table I at different catalyst composition and concentrations in this work.

Using the nonlinear least-squares method, the rate constants in Eqs. (16)–(21) can be obtained by minimizing Eq. (15). In Eqs. (16)–(20), it can be seen that there are seven rate constants to be determined, that is, k_1–k_7. According to the elementary steps, k_1 is related to the decarboxylation of the carboxylic group in alkyl aromatics, and k_2 to the destruction of acetates. Both of them are influenced by the concentrations of high-valent transition metals. k_3–k_5 are concerned with the generation and decomposition of the intermediate $HOOCH_2COOH$. k_6 and k_7 are for the decomposition of the phenol to CO_2 and CO, respectively. So, k_3–k_7 are independent of catalyst concentrations. In the determination of k_1–k_7 with different catalyst concentrations, k_1 and k_2 are the two adjustable parameters but k_3–k_7 should be constant.

Figures 3–6 present the comparisons between the experimental and calculated data for CO_2 and CO formation in different catalyst conditions. It can be seen that for CO_2 the measured values increase almost linearly in the earlier stage and subsequently reach a plateau. The calculated values are in good agreement with the experiments. The disagreement should be due to the following reasons. First, some unknown elementary steps contributing to the formation of CO_2 were not involved in the model. Next, k_1 is related to the concentration of high-valent transition metals, which

Table I Rate Constants for the Main Reaction of PX Oxidation at Different Catalyst Composition and Concentrations

[Co]/[Mn]/[Br] 10^{-6} (kg/kg)	$k_1 \times 10^5$ (min^{-1})	$k_2 \times 10^{-3}$ (kg mol^{-1}) min^{-1}	$k_3 \times 10^{-3}$ (kg mol^{-1} min^{-1})	$k_4 \times 10^{-3}$ (kg mol^{-1} min^{-1})	$k_5 \times 10^{-3}$ (kg mol^{-1} min^{-1})	k_6 (kg mol^{-1} min^{-1})
350/350/700	2.46 ± 0.14	15.88 ± 0.62	17.09 ± 0.53	3.28 ± 0.13	9.81 ± 0.28	0.54 ± 0.02
700/350/700	4.74 ± 0.33					
350/700/700	2.78 ± 0.24					
350/350/1400	2.58 ± 0.13					

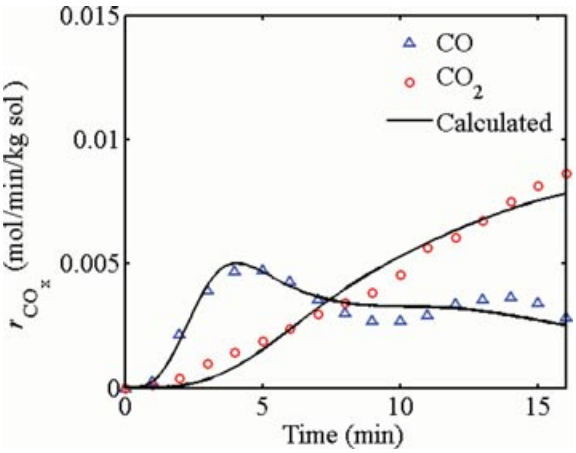

Figure 4 Model fitting to the formation rate of CO_x. [Co]/[Mn]/[Br]: 700/350/700 10^{-6} kg/kg; $T = 465$ K.

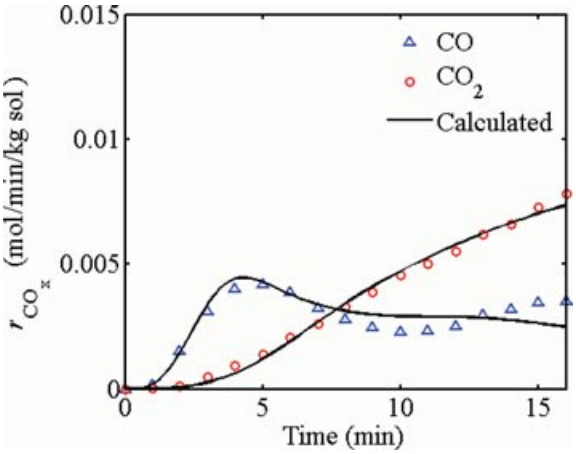

Figure 5 Model fitting to the formation rate of CO_x. [Co]/[Mn]/[Br]: 350/700/700 10^{-6} kg/kg; $T = 465$ K.

may be fluctuating during the formation of CO_x. To simplify, we assumed their concentrations to be constant.

It is shown that there are two peaks for CO formation as the function of time, and the first peak was captured successfully by the model in this work whereas the second was not. There should be other elementary steps contributing to the CO formation in the latter period, which were not considered in this work. Actually, we

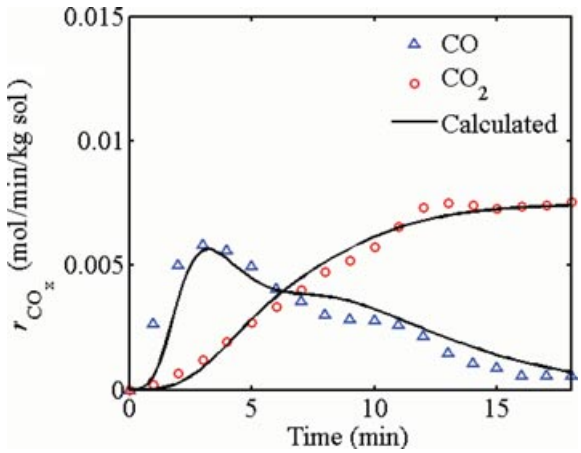

Figure 6 Model fitting to the formation rate of CO_x. [Co]/[Mn]/[Br]: 350/350/1400 10^{-6} kg/kg; $T = 465$ K.

tried to write down some elementary steps, which we believe are important for CO formation, and used them in the model, but the fitting results did not improve. Furthermore, the addition of these elementary steps made the confidence intervals of rate constants wider. As we all know, when the observed parameters are limited, the increase in the numbers of the nonkey model parameters usually leads to a wider confidence interval.

The summary of the rate constants k_1–k_7 is presented in Table II, along with the confidence intervals with the 95% confidence level. It can be seen that all of the rate constants are higher than their respective confidence intervals. Especially for k_1–k_6, their respective confidence intervals are one or two orders of magnitude less than the parameters. From the point of view of statistics, these parameters estimated from experiments are quite reasonable.

It should be pointed out that the values of k_1 or k_2 are not in proportion to the concentration of the metal components in the catalyst. This is because there is a complex synergy between the catalyst components such as Co, Mn, and Br in the presence of aromatic acids [3]. So the increase in one metal concentration does not mean the corresponding enhancement in its high-valent form.

Table II Summary of Rate Constants and Confidence Interval with 95% Confidence Level

[Co]/[Mn]/[Br] 10^{-6} (kg/kg)	k_1 10^{-3} (min^{-1})	k_2 10^{-3} (mol/min/kg sol)	k_3 (min^{-1})	k_4 (kg sol/mol/min)	k_5 (min^{-1})	k_6 (min^{-1})	k_7 (min^{-1})
350/350/700	0.74 ± 0.06	3.36 ± 0.03	7.06 ± 0.29	4.16 ± 0.14	0.16 ± 0.03	7.13 ± 0.92	0.42 ± 0.16
700/350/700	1.26 ± 0.12	3.88 ± 0.13					
350/700/700	1.25 ± 0.11	3.31 ± 0.45					
350/350/1400	1.06 ± 0.10	4.40 ± 0.02					

CONCLUSION

The HMBCA oxidation of PX was carried out under industrial conditions, and the formation kinetics of CO_x including CO_2 and CO was measured. The simplified elementary steps for CO_x formation were summarized, on the basis of which the kinetic model of CO_x formation was established.

According to the key elementary steps and model-fitting results, there are two sources for the formation of CO_2. One is from the aromatic acid, including the decarboxylation of the carboxylic group, and the complete decomposition of the quinone, which comes from the aryl radical generated during the decarboxylation. The other source is the destruction of the reaction solvent acetic acid, in which the carbon-centered radicals were first formed from acetic acid and subsequently converted to CO_2 and CO. The destruction of acetic acid is one of the major sources of CO. Another part of CO comes from the complete decomposition of the quinone.

For the formation of CO_2, the fitting curve is in good agreement with the experimental data. There are two peaks for the formation rate of CO as a function of time, in which the first is captured successfully by the model. The rate constants of the key elementary steps were determined with narrow confidence intervals.

BIBLIOGRAPHY

1. Suresh, A. K.; Sharma, M. M.; Sridhar, T. Ind Eng Chem Res 2000, 39, 3958.
2. Partenheimer, W.; Gipe, R. K. In Catalytic Selective Oxidation; Oyama, S. T.; Hightower, J. W., Eds.; American Chemical Society: Washington, D.C., 1993; p. 81.
3. Partenheimer, W. In Catalysis of Organic Reactions; Blackburn D. W., Ed.; Marcel Dekker: New York, 1990; p. 321.
4. Partenheimer, W. Catal Today 1995, 23, 69.
5. Roffia, P.; Calini, P.; Motta, L. Ind Eng Chem, Prod Res Dev 1984, 23, 629.
6. Ariko, N. G. Kinet Catal 1991, 32, 757.
7. Kenigsberg, T. P.; Ariko, N. G.; Agabekov, V. Energy Convers Manage 1995, 36, 677.
8. Kenigsberg, T. P.; Ariko, N. G.; Mitskevich, N. I.; Nazimok, V. F. Kinet Catal 1985, 26, 1279.
9. Sun, W.; Zhao, L. Ind Eng Chem Res 2011, 50, 2548.
10. Sun, W.; Pan, Y.; Zhao, L.; Zhou, X. Chem Eng Technol 2008, 31, 1402.
11. Chen, D.; Sun, W.; Pan, Y.; Zhao, L. Petrochem Technol 2006, 35, 1105.
12. Li, J.; Brill, T. B. Int J Chem Kinet 2003, 35, 602.
13. Li, J.; Brill, T. B. J Phys Chem A 2003, 107, 2667.
14. Partenheimer, W. Adv Synth Catal 2005, 347, 580.
15. Alzueta, M. U.; Glarborg, P.; Dam-Johansen, K. Int J Chem Kinet 2000, 32, 498.
16. Sheldon, R. A. In Catalytic Oxidation; Sheldon, R. A.; Santen, R. A. v., Eds.; World Scientific: Singapore, 1995; p. 151.